

## Full Length Research Paper

# Thermo-chemical sequestration of naphthalene using *Borassus flabellifer* Shell activated carbon: Effect of influencing parameters, isotherm and kinetic study

J. Aravind Kumar<sup>1\*</sup>, D. Joshua Amarnath<sup>1</sup>, S. Anuradha Jabasingh<sup>2</sup> and S. Sathish<sup>1</sup>

<sup>1</sup>Department of Chemical Engineering, Sathyabama University, Chennai, Tamil nadu, India.

<sup>2</sup>Process Engineering Division, School of Chemical and Bio Engineering, Addis Ababa Institute of Technology, Addis Ababa, Ethiopia.

Received 6 September, 2016; Accepted 28 October, 2016

The present research describes the removal of naphthalene from aqueous solution using one of the simplest agricultural wastes, *Borassus flabellifer* Shell activated carbon (BFS-AC) by adsorption. Adsorption was chosen due to its cost-effectiveness. The effect of operating parameters such as pH, time, initial concentration of naphthalene, BFS-AC dosage and temperature on the percent removal of naphthalene was determined. The optimum conditions obtained were pH of 7, contact time of 12 h for an optimum concentration of 200 mg/L with the addition of 8 g at a temperature optimum at 40°C attaining the maximum percent removal. The adsorption kinetics supported the Freundlich model with R<sup>2</sup> value of 0.995 indicating multilayer adsorption. The chemical kinetic studies followed the pseudo second order mechanism. The characterization of BFS-AC was carried out using scanning electron microscopy (SEM) and X-ray diffraction (XRD) which showed the enhanced porosity and crystallinity of the adsorbent which was mainly due to the surface modification carried out by chemical addition followed by thermal treatment. The initial and final naphthalene concentration after adding the adsorbent was determined by using gas chromatography-mass spectrometry (GC-MS). The characterization thoroughly suggests the efficacy of *B. flabellifer* shell to efficiently sequester naphthalene from aqueous solution.

**Key words:** Naphthalene, *Borassus flabellifer*, thermo-chemical, activated carbon, adsorption.

## INTRODUCTION

Poly-aromatic hydrocarbons (PAHs) are structurally related chemicals consisting of aromatic rings with no substitutions. They are considered to be a very potent class of environmental pollutant causing harmful effects to the environment, which are found out in various environmental conditions (Kafilzadeh, 2015). Global

industrialization threatens the globe due to the uncontrolled usage and abuse of chemicals along with the exploitation of natural resources. Rapid industrialization resulted in dumping of large amount of chemical wastes into the environment as well as water resources. Petroleum waste is composed of many

\*Corresponding author. E-mail: arvindhjsbu@gmail.com.

fractions which includes PAHs as a major constituent (Clinton et al., 2014). The level of PAHs increases due to day to day activities such as mass traffic and variety of industrial processes (de Boer and Wagelmans, 2016). PAHs are the outcomes of various sources such as coal, fossil fuel and peat burning along with mobile sources in the urban regions (Moradi-Rad et al., 2014). PAHs were accumulated in all habitats of environment such as air, water, soil, and food. Many methods were available for the PAHs removal which includes absorption, biodegradation, ion exchange, chemical precipitation, and high energy irradiation (Balati et al., 2012). The use and management of environment is an important task today (Abdel-Shafy and Aly, 2002). Hence, the contamination of harmful pollutants in environment has become a serious issue, particularly in urban cities where there is more amount of water scarcity. With this aspect, drinking water is said to be contaminated with small amounts of various synthetic compounds which are rich in organic or inorganic contents (Moradi-Rad et al., 2014). Waste waters undergo different stages of treatment which includes primary to tertiary methods depending on availability of source to meet the environmental standards. Anyway, the organic waste such as PAHs are not easily removed with such treatment techniques (Alade et al., 2012). The hydro-phobic nature of PAHs resulted in more amount of toxicity to the environment (Jorfi et al., 2013). The toxic nature, mutagenic and carcinogenic characteristics of PAHs categorized them to be primary pollutants. PAHs are adsorbed easily due to their less solubility tendency in aqueous solutions (Lamichhane et al., 2016). Many compounds were selected as representatives of PAHs, but this study is focused on naphthalene. Naphthalene is present abundantly in waste water, obtained from various industrial activities (Ania et al., 2007). Naphthalene was investigated to be one of the most prominent PAHs in waste water. Naphthalene removal can be carried out using many methods (Aisien et al., 2014) out of which adsorption is found to be a convenient one.

Agricultural materials were found to be more predominant to act as adsorbents due to less cost, large availability and high sorption capacity (Zhu et al., 2016; Pal, 2012). Excess amount of waste materials are generated in the form of agricultural materials such as coconut, corn and palm shell *Borassus flabellifer* (Kumar et al., 2015). *B. flabellifer*, also called Asian palmyra palm, toddy palm, or sugar palm, is native to Indian Subcontinent (Vijayalakshmi and Rajalakshmi, 2010). It is a robust tree, reaching a height of 30 m. The trunk is grey, robust, ringed with leaf scars. The leaves are fan-shaped, 3 m in length. Palm shell is the dried fruit of *B. flabellifer* and it is an agricultural solid material. This is available in plenty from the mills and can be considered as an excellent raw material for the production of activated carbon (Charlesworth et al., 2002; Boving and Zhang, 2004; Ozer and Ozer, 2004; Ayranci, 2005; Tan et al., 2008). Activated carbon has a wide range of

applications including the removal of unpleasant odor, taste, color, impurities from domestic and industrial effluents (Kent, 1992; Cooney, 1999; Amarnath and Padmesh, 2009; Yu et al., 2012; Mohan and Singh, 2002; Liao et al., 2011; Momčilović et al., 2011). Activated carbon produced from *B. flabellifer* shell was observed to possess large surface area and pore volume. This feature facilitates its application as an effective adsorbent (Momčilović et al., 2011). Though many activating agents are employed by many researchers for the pretreatment process which involves, carbonization and activation, the present study employs zinc chloride and potassium hydroxide as an activating agent (Jabasingh et al., 2015) followed by thermal pyrolysis.

The precursors include various coal and other biologically derived materials. The activated carbon obtained were subjected to thermal treatment which resulted in the formation of char and other gases (Prabu et al., 2015; Kiruba et al., 2014). This char was able to act as an excellent precursor in the synthesis of activated carbons (Cabal et al., 2009). This study involves the combination of chemical (Gaya et al., 2015) and thermal treatment which was found to be the first in adsorbent preparation. The selection of *B. flabellifer* shell (BFS) mainly depends on the fact that it is much denser when compared with other biological materials (Okoroigwe et al., 2014).

## EXPERIMENTAL

### Materials

Naphthalene (98% pure), potassium hydroxide (97% pure), zinc chloride (95% purity), and acetone were purchased from Sigma Aldrich, Germany. The stock solution of naphthalene was prepared using acetone and distilled water. The acetone water solution was used to enhance the hydrophobic solubility nature of naphthalene (Felixa et al., 2014). The primary material for activated carbon preparation, *B. flabellifer* shells were procured from Godrej palm plantations, Salem, Tamilnadu, India after palm fruit extraction.

### BFS-AC preparation

*B. flabellifer* shells are collected, washed with distilled water, and dried in oven at 100°C. The dried materials were chopped finely and sieved to mesh size of 2 mm. The resulting materials are subjected to drying at 400°C for 2 h in muffle furnace. After drying, the materials are soaked in 3% KOH solution and 2% ZnCl<sub>2</sub> in a ratio of 1:3 for impregnation of the activating agent (Gaya et al., 2015). The chemical activation enhanced the surface area and pore volume to a maximum extent which was confirmed by scanning electron microscopy (SEM) and X-Ray diffraction (XRD) analysis. The impregnation process is followed by thermal treatment at 600°C for 2 h in a muffle furnace. The dried sample is washed repeatedly with de-ionized water until neutrality was attained. The samples are further dried at 200°C for 4 h in a tray dryer to remove the excess moisture content. This treatment was found to be the first one when compared with earlier strategies. This is named as *B. flabellifer* shell activated carbon (BFS-AC) and stored in sealed containers. BFS-AC is used in the present study for the removal of naphthalene from aqueous solution.

## Physical and chemical characterization of BFS-AC

### Moisture content determination

An empty crucible was weighed and 1 g of BFS-AC was added and the weight of the crucible along with BFS-AC was measured. The BFS-AC loaded crucible was dried in the air oven at 105°C for 24 h and placed in desiccators. The weight of the dried BFS-AC was measured. The moisture content was calculated as follows:

$$\%M = \frac{(W_A - W_C)}{(W_B - W_C)} \times 100 \quad (1)$$

where  $W_A$ ,  $W_B$  and  $W_C$  are the empty weight of the container, initial weight of the container with BFS-AC, and final weight of the container with BFS-AC, respectively.

### Ash content determination

An empty crucible was weighed and 1 g of BFS-AC was added to it and the weight of empty crucible along with the BFS-AC was measured. The BFS-AC loaded crucible was dried in a muffle furnace for 2 h at 550°C and kept in desiccators for 30 min followed by measuring the weight. The ash content was calculated as follows:

$$\%A = \frac{(W_B - W_C)}{(W_B - W_A)} \times 100 \quad (2)$$

where  $W_A$ ,  $W_B$  and  $W_C$  are the empty weight of the container, initial weight of the container with BFS-AC, and final weight of the container with BFS-AC, respectively.

### Batch adsorption studies

Stock solution of naphthalene was prepared by dissolving 1 g of naphthalene in 1 L acetone. Diluted concentration of 100, 200, 300 and 400 ppm were prepared from the stock using acetone and distilled water. Batch experiments were conducted in 100 ml conical flasks in a laboratory shaker at 200 rpm in order to determine the effect of pH (2 to 8), temperature (30 to 50°C), time (1, 2, 3, 4, 6, 18 and 20 h), BFS-AC dosage (2 to 8 g/L) and initial concentration of naphthalene (100 to 400 mg/L) on the percentage naphthalene sorption from aqueous solution using BFS-AC. The added adsorbent was separated by centrifuge at 500 rpm. The supernatant was filtered through a 0.45 mm membrane filter and analyzed quantitatively at various time intervals for naphthalene concentration. Supernatant samples after adsorption were subjected to Gas Chromatography–Mass Spectrometry (GC-MS) analysis using purge and trap, GCMATE II GC-MS. GC-MS analysis for detecting naphthalene concentration before and after adsorption was determined by the CMIP5 instrument 210 series equipped with a 100 m Fison DB-5 capillary column operating at a temperature range of 120°C in the splitless mode with an injection volume of 1 µl/min. The adsorption percentage of naphthalene was calculated from the differences between the concentrations of naphthalene in the aqueous solution before and after adsorption process (Jabasingh et al., 2015).

$$\text{Adsorption } \% = \frac{C_0 - C_f}{C_0} \times 100 \quad (3)$$

## Adsorption isotherms

The adsorption isotherms were studied in order to show the adsorption behavior and to determine the adsorption capacity. Langmuir and Freundlich adsorption isotherms were fitted to the experimental results for the adsorption of naphthalene. Both isotherms indicate a sharp initial slope indicating the high efficiency of the adsorbent at low concentration and saturation at high concentration (Jabasingh et al., 2010). The linear form of Langmuir isotherm is given by

$$\frac{1}{q_{eL}} = \frac{1}{q_M} + \frac{1}{C_E K_L q_M} \quad (4)$$

And the linear form of Freundlich equation is given by

$$\log q_{eF} = \log K_F + \frac{1}{n} \log C_e \quad (5)$$

where  $q_{eL}$ ,  $q_{eF}$  and  $q_M$  are the equilibrium adsorption capacity (mg g<sup>-1</sup>) according to Langmuir fit, equilibrium adsorption capacity (mg g<sup>-1</sup>) according to Freundlich fit and the maximum sorption capacity (mg g<sup>-1</sup>), respectively.  $K_L$  (ml mg<sup>-1</sup>) and  $K_F$  (mg g<sup>-1</sup>) are the Langmuir and Freundlich constants, respectively.  $C_e$  and  $n$  are equilibrium naphthalene concentration (mg/L) and sorption intensity, respectively.

## Chemical kinetics

Kinetic study was carried out using 50 ml naphthalene solution in the concentration ranging from 100 to 400 mg/L with the addition of 8 g of activated carbon. The pseudo first order and pseudo second order kinetics were determined. A pseudo first order kinetics suggest a constant concentration of any one of the reactants as it is supplied in excess. The sorption kinetic data were treated with pseudo first-order model (Felixa et al., 2014).

$$\log(q_e - q_t) = \log q_e - \left[ \frac{k_1}{2.303} \right] t \quad (6)$$

where  $q_t$  is the sorption capacity of BFS-AC at any time  $t$  and  $k_1$  is the first order rate constant (min<sup>-1</sup>). The pseudo second order kinetics depend on two reactants and the equation is given as:

$$\frac{t}{q_t} = \frac{1}{k_2 q_e^2} + \left[ \frac{1}{q_e} \right] t \quad (7)$$

Where,  $k_2$ (g/mg min) is the second order rate constant, determined from the plot of  $t/q_t$  versus  $t$ . The initial sorption rates were given by

$$h = k_2 q_e^2 \quad (8)$$

## Thermodynamic studies

The enthalpy, entropy and Gibbs free energy values were determined using

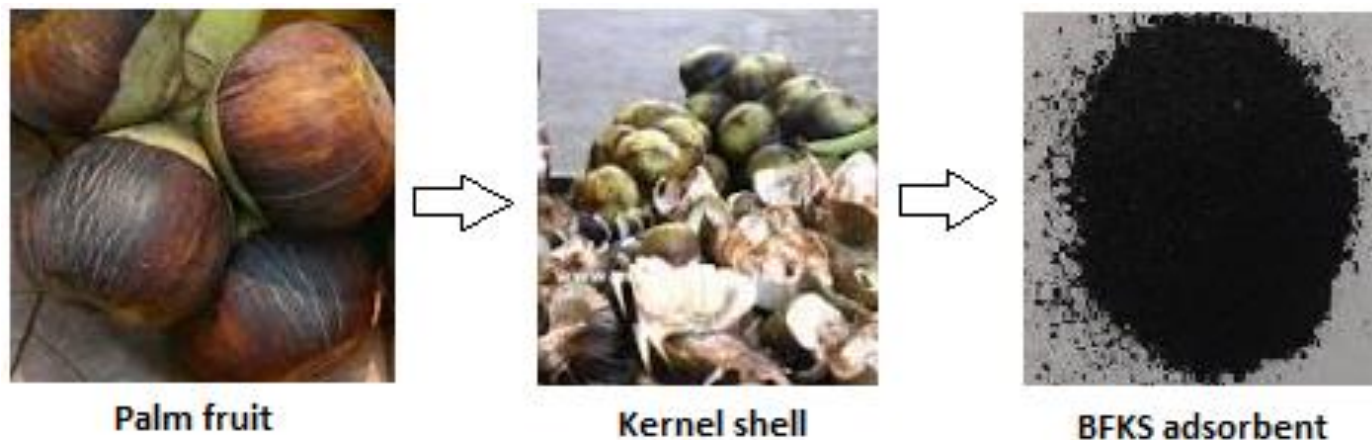


Figure 1. Preparation of BFS-AC.

$$K_D = \frac{q_e}{C_e} \quad (9)$$

$$\log K_D = \frac{-\Delta G}{2.303RT} = \frac{-\Delta H}{2.303RT} + \frac{\Delta S}{2.303R} \quad (10)$$

where  $K_D$  is the distribution coefficient in  $\text{ml mg}^{-1}$ .  $\Delta H$ ,  $\Delta S$  and  $\Delta G$  are changes in enthalpy, entropy and Gibbs free energy, respectively (Kiruba et al., 2014).

#### Analytical methods

The surface morphology of BFS-AC was studied using scanning electron microscope, SEM Supra 55 Carl Zeiss, Germany. The crystallinity of BFS-AC was determined using X-ray diffraction analysis. XRD analysis of the BFS-AC was carried out by the Rigaku laboratory equipment maintained at a voltage of 30 Kv and a current of 20 MA Cu-K $\alpha_2$  radiations. Determination of naphthalene before and after the adsorption process was carried out using GC-MS (CMIP5 instrument 210 series) with a capillary DB-5 column. Naphthalene was quantified using calibration curves by the direct injection of standard mixtures with known concentrations.

## RESULTS AND DISCUSSION

### Characterization of BFS-AC

Figure 1 shows the activated carbon produced from *B. flabellifer* Shell. The ash content and moisture content of BFS-AC was found to be 10.9 and 3.4%, respectively.

SEM images (Figure 2a to c) show the morphology of the initial shell, shell after its conversion to activated carbon (BFS-AC), BFS-AC after adsorption of naphthalene. Large sized pores developed on the shell after the activation process during its conversion to activated carbon. The KOH activation and pyrolysis processes have increased the pore size and pore volume due to the

diffusion of KOH and CO $_2$ . This reaction has also resulted in the drastic expansion of the carbon material. The surface of BFS-AC looked like a honeycomb before adsorption process. After the adsorption of naphthalene, the pores were found to expand in their capacity. The fringes disappear after the adsorption process, showing the affinity of naphthalene towards BFS-AC.

Figure 3 gives the crystalline nature and composition of the BFS-AC sample before adsorption of naphthalene. The diffractograms obtained are similar and in better agreement with the XRD pattern of the sample. But, the undesirable peaks in the pattern confirmed the presence some amount of impurity in the sample. XRD indicated the powder pattern of the derived activated carbon under atmospheric conditions. The broad peaks at 2 $\theta$ , 26.5°, 27.9°, 28.1°, and 28.8° and the peaks at 34.5° and 35.1° confirmed the presence of activated carbon. XRD predicts the particle size of the BFS-AC sample in the range of 2 to 3 nm. GC-MS was used to detect the presence of low molecular weight, naphthalene in aqueous solution before and after the addition of BFS-AC. The reduction in peak confirmed the removal of naphthalene after the addition of adsorbent. Figure 4a and b shows the GC-MS spectra of the naphthalene solution before and after adsorption using BFS-AC.

### Effect of various operating parameters

The results of the effect of various operating parameters on naphthalene removal percentage are as shown in Figure 5. The effect of initial naphthalene concentration was determined between 100 and 400 mg/L. The adsorption percentage increases with an increase in the amount of the adsorbent due to the large availability of vacant sites for adsorption. The percentage adsorption was found to decrease beyond 200 mg/L, due to the complete occupation of the vacant sites by naphthalene

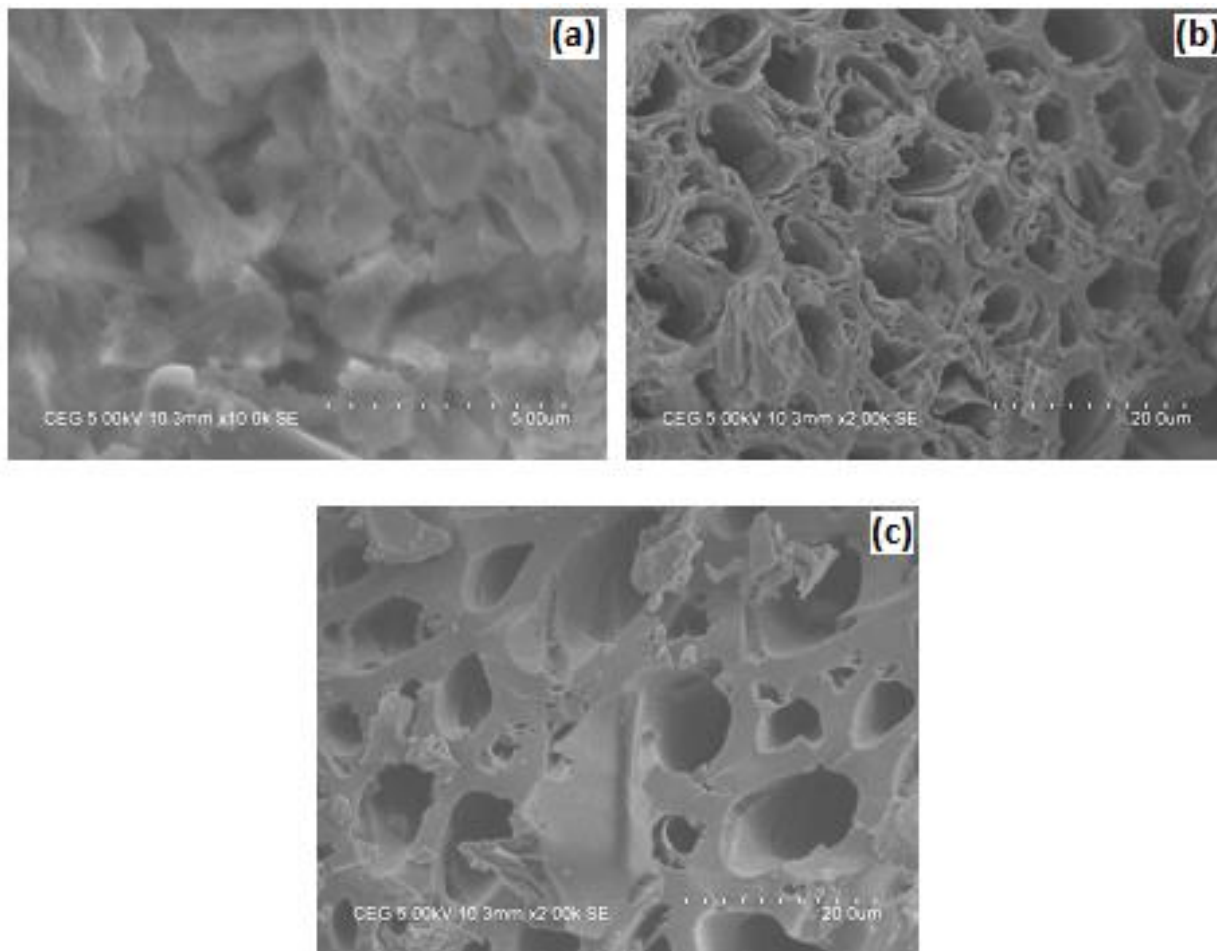


**Figure 2.** SEM morphology of (a) *Borassus flabellifer* shell, (b) BFS-AC before the adsorption of naphthalene, (C) BFS-AC after adsorption of naphthalene.

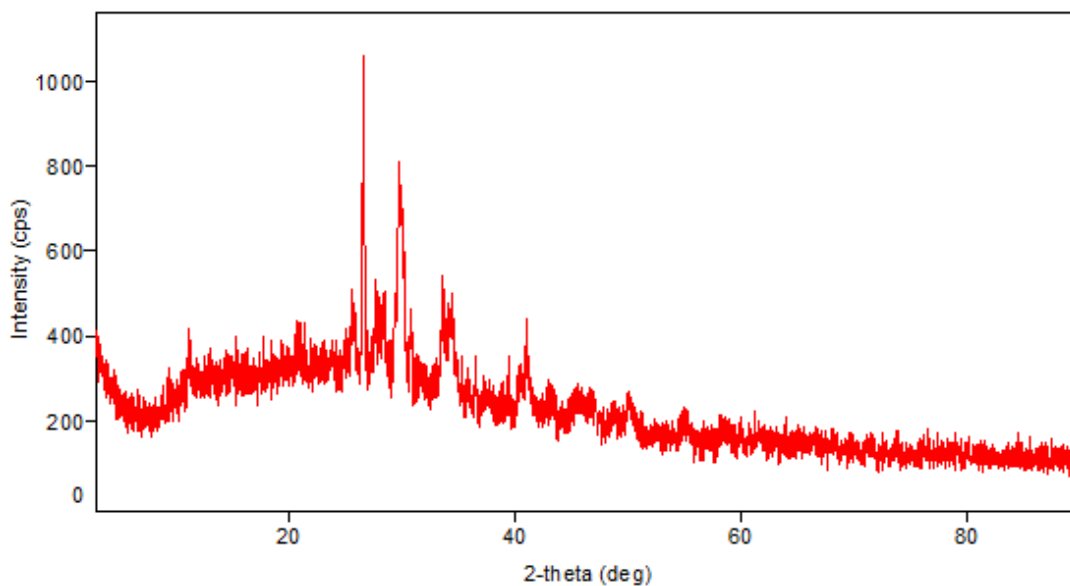


**Figure 3.** XRD pattern of BFS-AC.

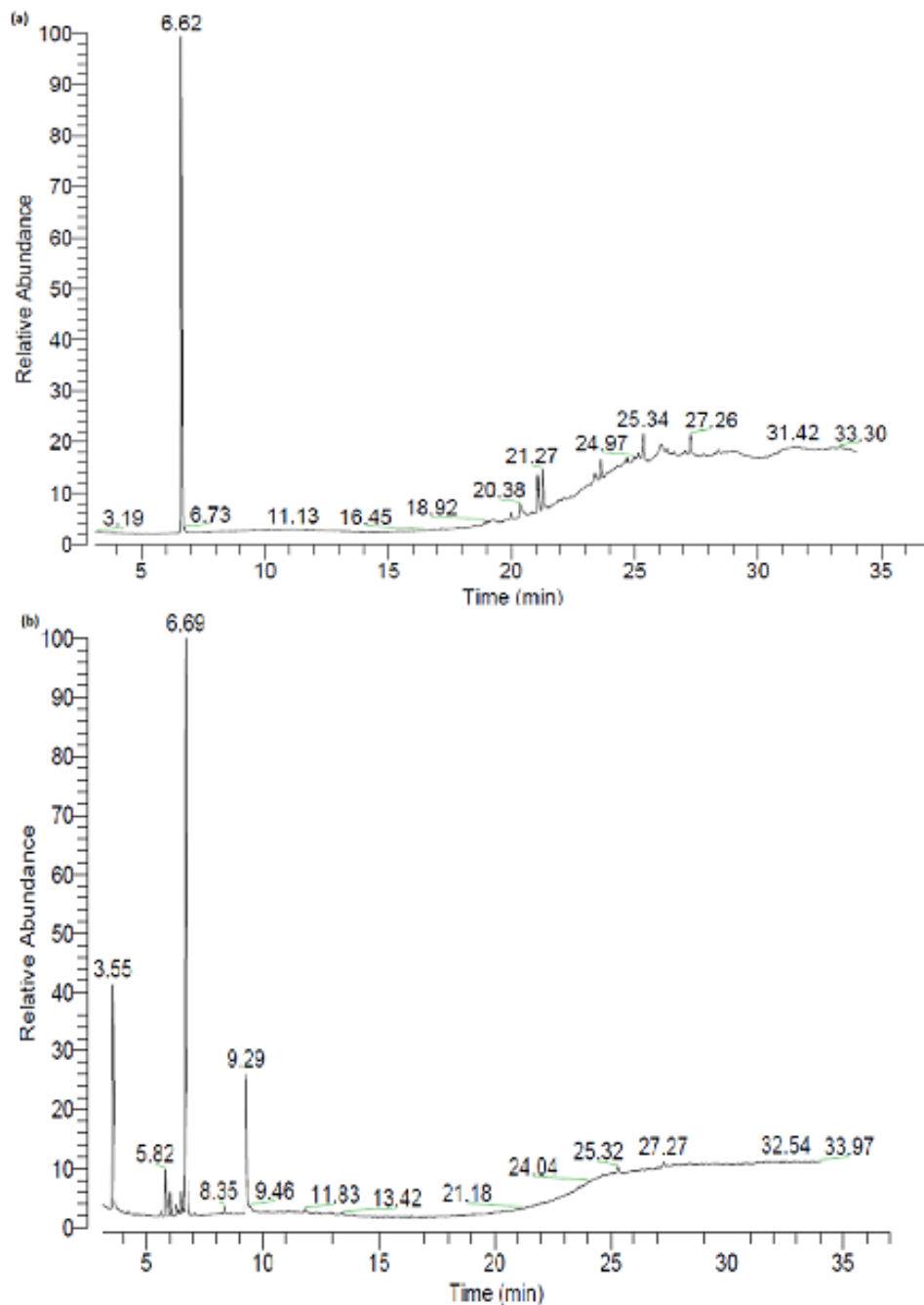


**Figure 4.** GC-MS spectra of the solution (a) before adding BFS-AC (b) after adsorption using BFS-AC.

molecules. The effect of pH was determined for the solution of concentration 200 mg/L. The solution was tested at various pH levels in the range of 3 to 9. Low pH increased the concentration of  $H^+$  ions and higher pH increased the concentration of  $OH^-$  ions. It was clear that increase in pH resulted in more concentration of  $OH^-$  ion in naphthalene solution (Momčilović et al., 2011; Jabasingh et al., 2015). More ionized form resulted in less

adsorption. The adsorption was maximum at a pH of 7. At this pH, more hydrogen ions were present and this has made the improvement in the activation process by means of triggering the carboxyl groups that are present in the activated carbon. Adsorption was carried out at various temperatures, 30, 35, 40, 45 and 50°C. It was found that as the temperature increases, the adsorption of naphthalene by BFS-AC increased and remained

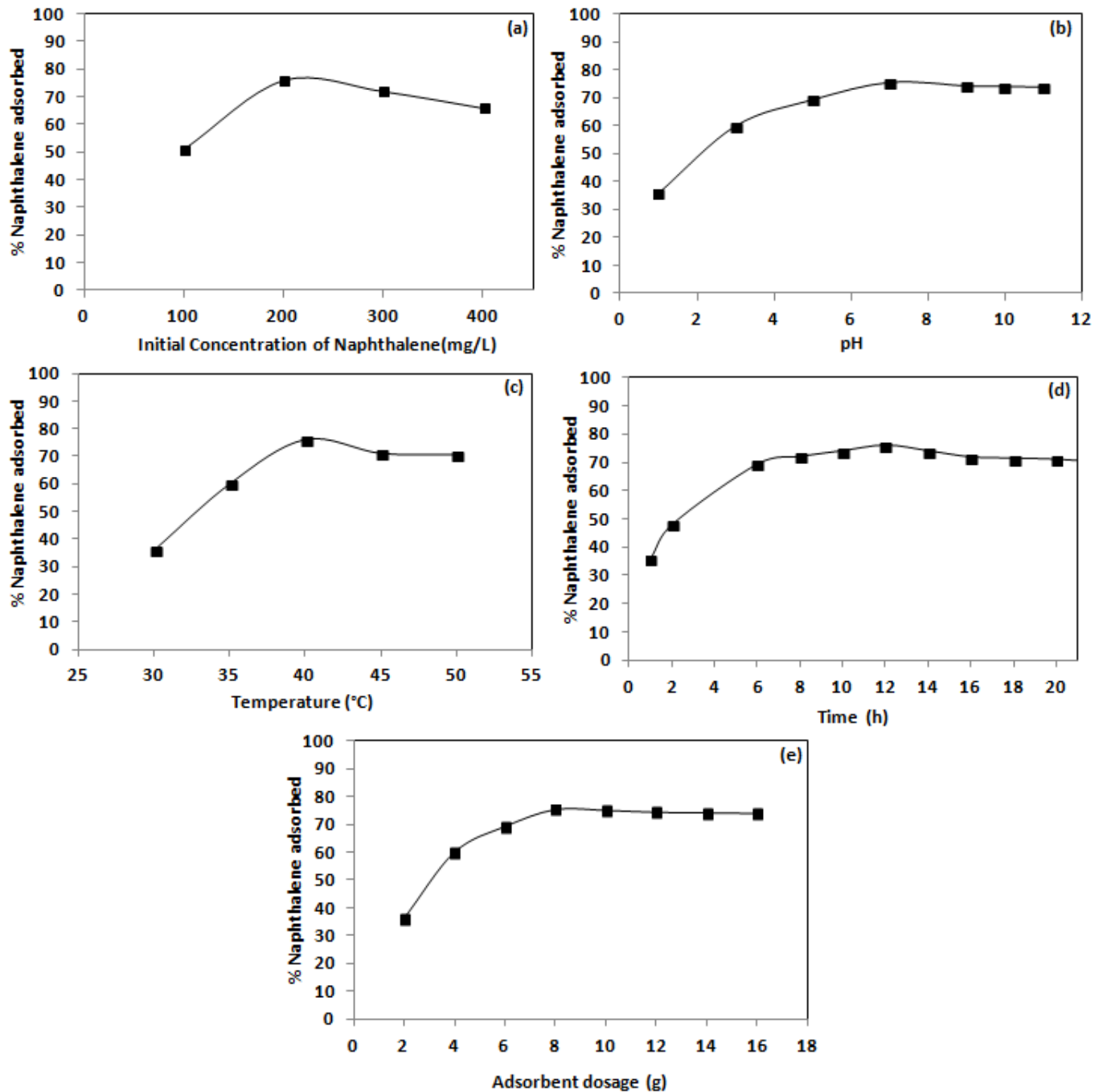


**Figure 5.** Effect of various operating parameters on naphthalene removal percentage.

constant at 40°C. The samples were subjected to adsorption at different time intervals of 1, 2, 4, 6, 12, 18 and 20 h. The optimum time for naphthalene adsorption by BFS-AC was found to be 12 h with a removal efficiency of 76%. Various dosages of BFS-AC including 2, 4, 6, 8, 10 and 12 g were added to the naphthalene solution of various concentrations. The optimum BFS-AC dosage was found to be 8 g. In order to determine the

effect of initial naphthalene concentration on the percentage removal, the naphthalene concentration was varied in the range of 100 to 400 mg/L with a dosage of 8 g adsorbent. At a high naphthalene concentration, the naphthalene molecules present on the surface was high and hence the functional adsorption was dependent on the concentration of initial amount of naphthalene.

Optimum initial concentration of naphthalene that can

**Table 1.** Adsorption isotherm parameters for naphthalene removal by BFS-AC.

Isotherm model	Parameter	Values	R <sup>2</sup>
Langmuir	q <sub>m</sub> (mg/g)	0.2256	0.9979
	K <sub>L</sub> (L/mg)	16.036	
Freundlich	K <sub>F</sub> (L/mg)	0.2455	0.9271
	n (g/L)	4.114	

be effectively adsorbed by BFS-AC was found to be 200 mg/L. Beyond this concentration, the removal percentage was found to decrease.

### Adsorption isotherms

The adsorption isotherms were studied in order to show the adsorption behavior and to estimate the adsorption capacity. The fit of Langmuir and Freundlich adsorption isotherms to the experimental results for the adsorption of naphthalene are obtained. Both isotherms indicate a sharp initial slope indicating that the adsorbent operates at high efficiency at low concentration and becomes saturated at high adsorbent concentrations. The Freundlich constant, *n*, is a measure of both the relative magnitude and diversity of energies associated with the adsorption of naphthalene on palm shells. The adsorption isotherm was used to explain the distribution of solute particles between the liquid and solid phase when an equilibrium state was achieved for the adsorption process. The fitting of the experimental data to the different isotherm equations was an important task in order to find an exact model which is applicable for design purposes. Adsorption isotherms describe the interaction of solutes with the adsorbents and it finds an important application in optimizing the parameters to determine the equilibrium state. Langmuir isotherm describes the monolayer formation and energy term in this equation is expressed as a function of surface coverage. The values of K<sub>L</sub> and q<sub>M</sub> are listed in Table 1. The popular form of logarithmic equation was related with Freundlich isotherm and this holds good for multilayer formation on the solid surface. The Freundlich constants, K<sub>F</sub> and *n* values are listed in Table 1. The Langmuir and Freundlich isotherms were validated with their correlation coefficient. The Langmuir isotherm was found to fit the experimental data. Langmuir and Freundlich plots are as shown in Figure 6a and b, respectively.

### Adsorption kinetics

The pseudo first order and pseudo second order reaction kinetic constants were evaluated naphthalene adsorption (Table 2). The kinetics of naphthalene adsorption quietly

agreed with the pseudo-second order. The controlling step for the pseudo second order was chemisorption mechanism which resulted in the exchange of electrons between the solute particles and solvent (Nasernejad et al., 2005). The results confirmed well to the pseudo second order model equation. If the concentration of one of the reactants remains constant due to its supply in excess, the kinetics could be described as pseudo first order. The second order reaction depends on two reactants (naphthalene and BFS-AC). The pseudo first order and pseudo second order reaction kinetics for naphthalene adsorption onto BFS-AC is as shown in Figure 7a and b.

### Adsorption thermodynamics

Enthalpy, entropy and Gibbs free energy values for the naphthalene adsorption onto BFS-AC are shown in Table 3. The thermodynamic parameters ( $\Delta H$ ,  $\Delta S$  and  $\Delta G$ ) are used to determine the energy changes that occur during the adsorption process. They describe the thermodynamic behavior of naphthalene molecules onto BFS-AC (Figure 8). The feasibility of the adsorption process and its spontaneous nature was confirmed by the negative value of  $\Delta G$  (Prabu et al., 2015).  $\Delta G$  increases with the lowering of temperature. Adsorption was favorable at low temperatures.

Chemisorption was found to be predominant in this study. Since  $\Delta H$  is negative, the reaction was exothermic. The negative value of  $\Delta S$  indicates a less interaction with the solid-liquid interface and hence a reduction in the adsorption process. This could be improved by providing mild agitation to the adsorption vessel during the adsorption process. Since  $\Delta H^0$  are greater than  $T\Delta S^0$  for all concentrations of naphthalene at all temperatures, the adsorption process was very much influenced by the enthalpy changes compared to the entropy changes.

### Conclusion

The study exploited the efficiency of activated carbon derived from *B. flabellifer* shells for the removal of naphthalene from aqueous solution. Activated carbon obtained from *B. flabellifer* shells was found to be an



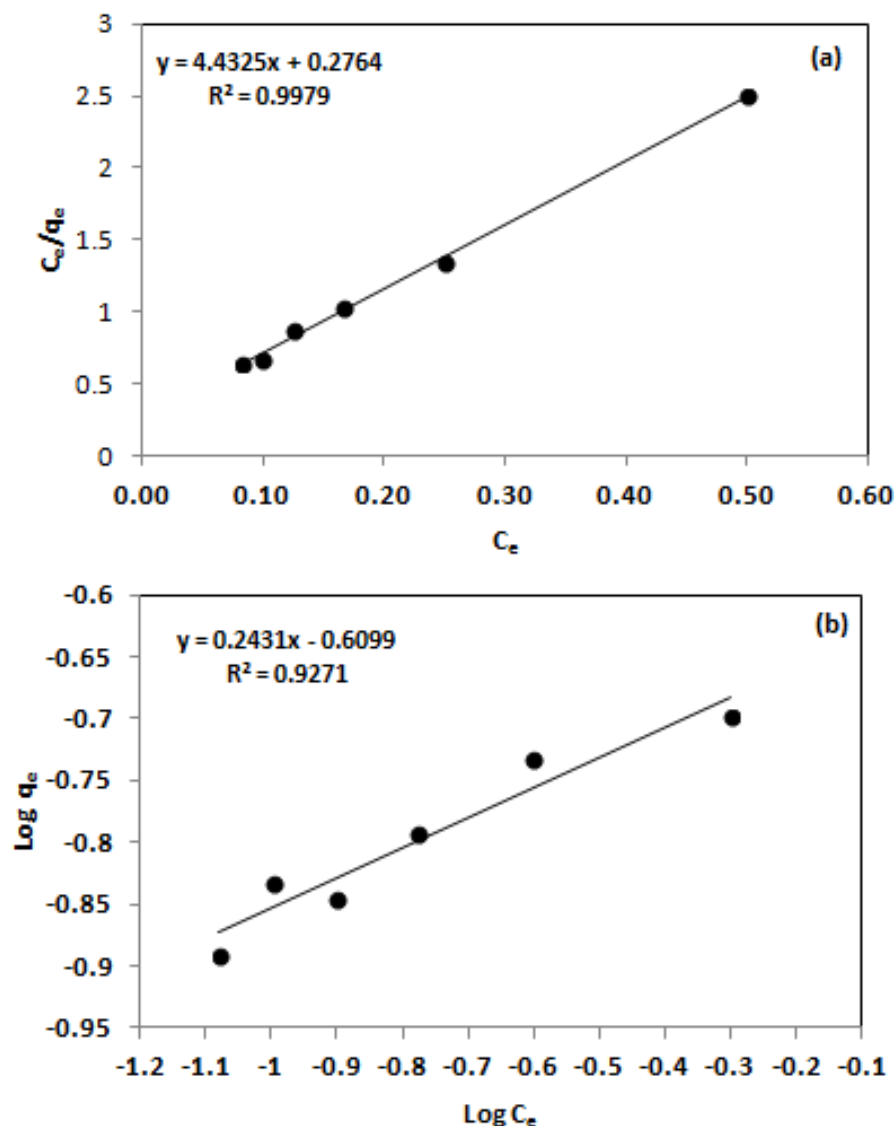


Figure 6. Experimental fit for (a) Langmuir isotherm, (b) Freundlich isotherm.

Table 2. Pseudo first order and pseudo second order adsorption kinetic constants at optimum naphthalene concentration.

Experimental		Pseudo first order kinetics			Pseudo second order kinetics		
$C_o$ (mg/L)	$q_{e(\text{exp})}$ (mg/g)	$k_1$ ( $\text{min}^{-1}$ )	$q_{e(\text{calc})}$ (mg/g)	$R^2$	$k_2$ (g/mg min)	$q_{e(\text{calc})}$ (mg/g)	$R^2$
200	10.5	0.153	3.855	0.991	0.088	7.299	0.996

excellent adsorbent for naphthalene removal from aqueous solution. The optimum conditions for the removal of naphthalene using *B. flabellifer* shells activated carbon were 8 g BFS-AC at a temperature of 40°C, at an optimum pH 7. This resulted in a maximum efficiency for BFS-AC to remove naphthalene from aqueous solution. Freundlich model provided a good fit to the experimental data with  $R^2$  value of 0.995. The

experiments proved a rapid adsorption of naphthalene by BFS-AC. A maximum adsorption capacity was achieved in approximately 12 h. The result of kinetic studies indicates the pseudo second order to be the best fitting kinetic model. The SEM analysis showed that the porosity of BFS-AC and XRD confirmed the crystalline nature of the BFS-AC. GC-MS analysis confirmed the adsorption of naphthalene by the adsorbent.

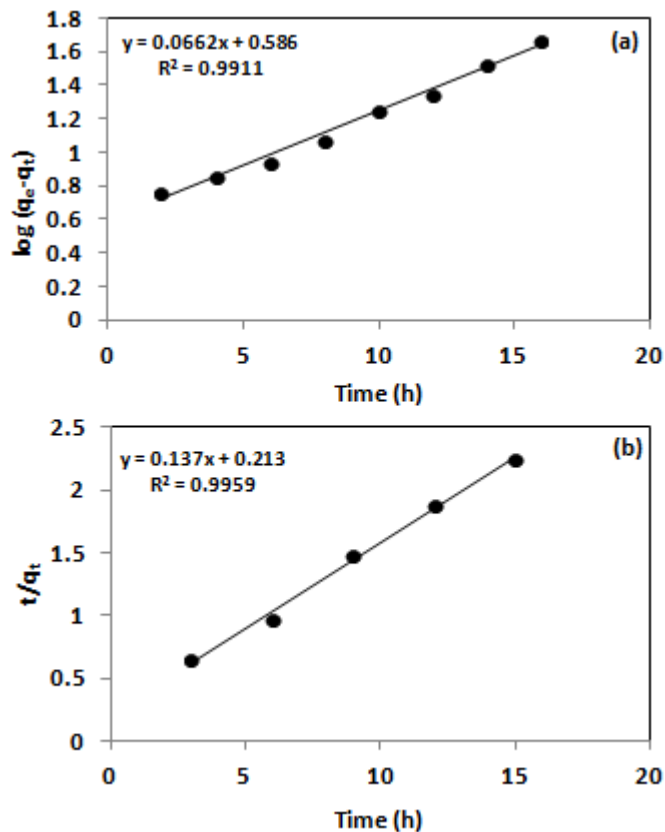


Figure 7. (a) Pseudo first order kinetics; (b) Pseudo second order kinetics.

Table 3. Enthalpy, entropy and Gibbs value for various concentrations of naphthalene

Initial concentration of naphthalene (mg/L)	$\Delta H^0$ (KJ/mol)	$\Delta S^0$ J/mol/K	$\Delta G^0$ (KJ/mol)
100	-608.13	-1164.13	-243.76
200	-544.31	-927.97	-253.86
300	-540.89	-889.15	-277.76

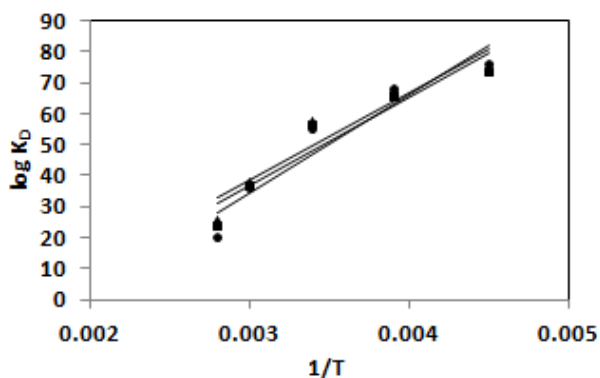


Figure 8. Thermodynamic plot for naphthalene adsorption onto BFS-AC.

### Conflict of interests

The authors have not declared any conflict of interests.

### REFERENCES

- Abdel-Shafy H, Aly R (2002). Water Issue in Egypt: Resources, Pollution and Protection Endeavors. Cent. Eur. J. Occup. Environ. Med. 8(1):3-21.
- Alade AO, Amuda OS, Jolaade AT, Ibrahim AO (2012). Isothermal studies of adsorption of acenaphthene from aqueous solution onto activated carbon produced from rice (*Oriza Sativa*) husk. Elixir Chem. Eng. 46:8461-8467.
- Amarnath RD, Padmesh TVN (2009). Adsorption of reactive orange 16 onto *Gracilaria* species a marine alga. Asian J. Chem. 21:4039-4046.

- Ania CO, Cabal B, Pevida C, Arenillas A, Parra JB, Rubiera F, Pis JJ (2007). Removal of naphthalene from aqueous solution on chemically modified activated carbons. *Water Res.* 41(2):333-340.
- Ayranci E (2005). Adsorption kinetics and isotherms of pesticides onto activated carbon-cloth. *Chemosphere* 60:1600-1607.
- Balati A, Shahbazi A, Amini MM, Hashemi SH, Jadidi K (2012). Comparison of the efficiency of meso-porous silica as absorbents for removing naphthalene from contaminated water. *Eur. J. Environ. Sci.* 4(1):69-76.
- Boving T, Zhang W (2004). Removal of aqueous phase polynuclear aromatic hydrocarbons using apen wood fibers. *Chemosphere* 54:839-881.
- Cabal B, Budinova T, Ania CO, Tsyntsarski B, Parra JB, Petrova B (2009). Adsorption of naphthalene from aqueous solution on activated carbons obtained from bean pods. *J. Hazard. Mater.* 161:1150-1156.
- Charlesworth M, Service M, Gibson GE (2002). PAHs contamination of Irish sediments. *Mar. Pollut. Bull.* 44:1421-1424.
- Clinton EI, Ngozi ON, Ifeoma OL (2014). Heavy Metals and Polycyclic Aromatic Hydrocarbons in Water and Biota from a Drilling Waste Polluted Freshwater Swamp in the Mgbede Oil Fields of South-South Nigeria. *J. Bioremediat. Biodegrad.* 5(7):21-28.
- Cooney DO (1999). *Adsorption designer for waste water experiment*, Lewis Publishers, London, 2:65-72.
- de Boer J, Wagelmans M (2016). Polycyclic Aromatic Hydrocarbons in Soil – Practical Options for Remediation. *Clean Soil Air Water* 44:648-653.
- Felixa A, Andrew A, Assogba M (2014). Heterogeneous photo-catalytic degradation of naphthalene using periwinkle shell ash: effect of operating variables, kinetic and isotherm study. *S. Afr. J. Sci.* 19(1):31-45.
- Gaya UI, Otene E, Abdullah AH (2015). Adsorption of aqueous Cd(II) and Pb(II) on activated carbon nanopores prepared by chemical activation of Doum palm shell. *Springer Plus* 4:458-475.
- Jabasingh SA, Lalith D, Garre P (2015). Sorption of Chromium (VI) from electroplating effluent onto Chitin immobilized *Mucor racemosus* sorbent (CIMRS) impregnated in Rotating Disk Contactor blades. *J. Ind. Eng. Chem.* 23:79-92.
- Jabasingh SA, Varma SS (2010). Optimization and Kinetic studies of Nickel treatment in the Electroplating effluent with Activated carbon prepared from Rice husk. *Indian Chem. Eng.* 52(3):230-247.
- Jorfi S, Rezaee A, Moheb-ali GA, alah Jaafarzadeh N (2013). Pyrene removal from contaminated soils by modified Fenton oxidation using iron nano Particles. *J. Environ. Health Sci. Eng.* 11(17):1-8.
- Kafilzadeh F (2015). Distribution and sources of polycyclic aromatic hydrocarbons in water and sediments of the Soltan Abad River, Iran. *Egypt. J. Aquat. Res.* 41:227-231.
- Kent JA (1992). *Riegel's handbook of industrial chemistry*, Van Nostrand Reinhold Publications, New York 1:442-455.
- Kiruba PU, Senthil KP, Sangita GK, Shahul HS, Sindhuja M, Prabhakaran C (2014). Study of adsorption kinetic, mechanism, isotherm, thermodynamic and design models for Cu(II) ions on sulphuric acid modified eucalyptus seeds: temperature effect. *Desalination Water Treat.* 22:26-35.
- Kumar JA, Amarnath DJ, Bowmick S (2015). Adsorption influence and isotherm studies for the removal of naphthalene using palm kernel shell. *Int. J. ChemTech Res.* 8(4):1912-1915.
- Lamichhane S, Krishna KB, Sarukkallige R (2016). Poly Aromatic Hydrocarbons (PAHs) removal by sorption – A review. *Chemosphere* 148:336-353.
- Liao SW, Lin CI, Wang LH (2011). Kinetic study on lead (II) ion removal by adsorption onto peanut hull ash. *J. Taiwan Inst. Chem. Eng.* 42:166-172.
- Mohan D, Singh KP (2002). Single and multi-component adsorption of cadmium and zinc using activated carbon derived from bagasse an agricultural waste. *Water Res.* 36:2304-2316.
- Momčilović M, Purenović M, Bojić A, Zarubica A, Randelović M (2011). Removal of lead(II) ions from aqueous solutions by adsorption onto pine cone activated carbon. *Desalination* 27:53-59.
- Moradi-Rad RO, Omid L, Kakooei H, Golbabaee F, Hassani H, Abedin-Loo RE, Azam K (2014). Adsorption of Polycyclic Aromatic Hydrocarbons on Activated Carbons: Kinetic and Isotherm Curve Modeling. *Int. J. Occup. Hyg.* 6:43-49.
- Nasernejad B, Zadeh TE, Pour BB, Bygi ME, Zamani A (2005). Comparison for bio-sorption modeling of heavy metals (Cr(III), Cu(II), Zn(II)) adsorption from wastewater by carrot residues. *Process Biochem.* 40:1319-1322.
- Okoroigwe EC, Saffron CM, Kamdem PD (2014). Characterization of palm kernel shell for materials reinforcement and water treatment. *J. Chem. Eng. Mater. Sci.* 5(1):1-6.
- Ozer A, Ozer D (2004). The adsorption of copper (II) ions onto dehydrated wheat bran (DWB): Determination of equilibrium and thermodynamic parameters. *Process Biochem.* 39(2):2183-2191.
- Pal D (2012). Adsorption of polycyclic aromatic hydrocarbons using s-effect of lignin content, International Conference of Chemical Ecology and Environmental Sciences, pp. 12-16.
- Prabu D, Parthiban R, Senthil Kumar P, Nupur K, Paharika S (2015). Adsorption of copper ions onto nano-scale zero-valent iron impregnated cashew nut shell. *Desalination Water Treat.* 2:1944-1952.
- Tan IAW, Ahmad AL, Hameed B (2008). Adsorption of basic dye using activated carbon prepared from palm shell-batch and fixed bed studies. *Desalination* 225:13-28.
- Vijayalakshmi PR, Rajalakshmi R, Subhashini S (2010). Inhibitory Action of *Borassus Flabellifer* (Palmyra Palm) Shell Extract on Corrosion of Mild Steel in Acidic Media. *E-Journal Chem.* 7(3):1055-1065.
- Yu F, Wu Y, Li X, Ma J (2012). Kinetic and thermodynamic studies of toluene, ethylbenzene and m-xylene adsorption from aqueous solutions onto KOH activated multiwalled carbon nano tubes. *J. Agric. Food Chem.* 60:12245-12253.
- Zhu M, Yao J, Dong L, Sun J (2016). Adsorption of naphthalene from aqueous solution onto fatty acid modified walnut shells. *Chemosphere* 144:1639-45.